4026 *Chem. Mater.* **2010,** *22,* 4026–4033
DOI:10.1021/cm100740n

CHEMISTRY OF MATERIALS
Article

Effects of Monomer Composition on CO_2−Selective Polymer Brush Membranes

Sebastian T. Grajales, Xiaojie Dong, Ying Zheng, Gregory L. Baker,* and Merlin L. Bruening*

Department of Chemistry, Michigan State University, East Lansing, Michigan 48824

Received March 12, 2010. Revised Manuscript Received May 11, 2010

Membranes that contain a high fraction of amorphous poly(ethylene glycol) (PEG) are attractive for selective removal of CO_2 from H_2 streams, but crystallization of PEG chains restricts both flux and selectivity. The high thickness of solution-cast membranes also limits flux. This study demonstrates the formation of composite, PEG-containing membranes through atom transfer radical polymerization of poly(ethylene glycol methyl ether methacrylate) from initiator-modified, porous substrates. The resulting membrane skins are only 50−500 nm thick, and copolymers that contain a mixture of short and long PEG side chains do not readily crystallize. The smaller PEG chains (8−9 ethylene oxide units) prevent crystallization, while the presence of longer side chains (23−24 ethylene oxide units) allows the membranes to maintain a CO_2/H_2 selectivity of 12 at room temperature. This work examines the effect of side-chain length on polymerization rate as well as the permeability, selectivity, and crystallinity of copolymer films. Reflectance FTIR spectroscopy reveals the fraction of different monomers incorporated into copolymer films and demonstrates when crystallization occurs.

Introduction

Selective removal of CO_2 from gas streams is becoming increasingly important for applications such as CO_2 sequestration,[1] fuel cell operation,[2] and H_2 synthesis.[3] In the case of H_2 production, steam reforming of methane produces 9 million metric tons of H_2 per year in the U.S. alone.[4] However, the product stream from steam reforming theoretically contains 20 mol % CO_2, so purification of the H_2 is an important and expensive part of the production process.[5] A number of studies examined membrane-based gas separation as a possible alternative, or as a prepurification step, to the pressure swing adsorption process currently used in H_2 purification.[6,7] The viability of membrane processes for purifying H_2 streams depends critically on achieving both high flux and high selectivity, and a recent review summarizes the types of membranes employed for H_2 purification.[8] Processes such as H_2 recycle in ammonia synthesis have employed H_2-selective membranes for several decades.[9] In the case of CO_2 removal from H_2 streams, however, CO_2-selective membranes are attractive because purified H_2 remains on the high pressure side of the membrane and does not need to be recompressed.

The solution diffusion model for transport through membranes (eq 1) illustrates how the flux, J, of a gas through a membrane depends on the pressure drop across the membrane, Δp, the membrane thickness, l, and the gas permeability, P, which is the product of the solubility coefficient, S, and diffusivity, D, for the gas of interest.[10] Equation 2 shows that the ideal selectivity of gas A over gas B, $\alpha_{A/B}$, depends on the solubility coefficients and diffusivities of the two gases. Because of its small size, H_2 has a greater diffusivity than CO_2, so CO_2/H_2 selectivity requires high solubility selectivity for CO_2 over H_2. Fortunately, CO_2 is the more condensable of the two gases, and solubility selectivity typically favors CO_2 transport.[10]

$$J = \frac{P\Delta p}{l} \quad P = SD \tag{1}$$

$$\alpha_{A/B} = \frac{P_A}{P_B} = \frac{S_A \times D_A}{S_B \times D_B} \tag{2}$$

Membrane materials employed for selective passage of CO_2 over H_2 should thus have a higher affinity for CO_2

*Corresponding authors e-mail: bruening@chemistry.msu.edu; bakerg@msu.edu.

(1) Scholes, C.; Kentish, S.; Stevens, G. *Sep. Purif. Rev.* **2009**, *38*, 1–44.
(2) Prakash, S.; Kohl, P. A. *J. Power Sources* **2009**, *192*, 429–434.
(3) Shao, L.; Low, B. T.; Chung, T. S.; Greenberg, A. R. *J. Membr. Sci.* **2009**, *327*, 18–31.
(4) U.S. Department of Energy, Energy Information Administration. The Impact of Increased Use of Hydrogen on Petroleum Consumption and Carbon Dioxide Emissions. http://www.eia.doe.gov/oiaf/servicerpt/hydro/pdf/oiafcneaf%2808%2904.pdf (accessed May 10, 2010).
(5) Molburg, J. C.; Doctor, R. D. *Proc. Ann. Int. Pitt. Coal Conf.* **2003**, *20*, 1388–1408.
(6) Favre, E. *J. Membr. Sci.* **2007**, *294*, 50–59.
(7) Lin, H. Q.; Van Wagner, E.; Freeman, B. D.; Toy, L. G.; Gupta, R. P. *Science* **2006**, *311*, 639–642.
(8) Ockwig, N. W.; Nenoff, T. M. *Chem. Rev.* **2007**, *107*, 4078–4110.
(9) Perry, E. Process for the Recovery of Hydrogen from Ammonia Purge Gases. U.S. Patent 4,172,885, Oct. 30, 1979.
(10) Kesting, R. E.; Fritzsche, A. K. *Polymeric Gas Separation Membranes*; John Wiley and Sons, Inc.: New York, 1993.

Published on Web 06/02/2010

Scheme 1. Methods for Growth of a Poly(PEGMEMA) Membrane from Porous Alumina

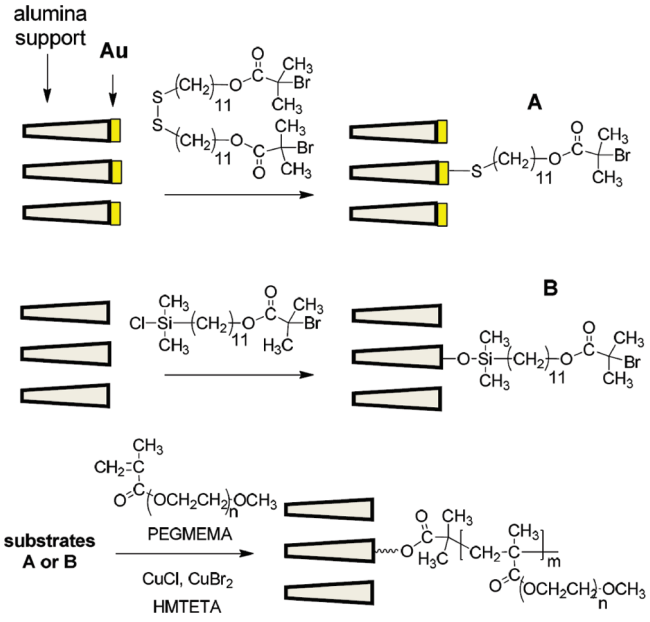

than H_2 along with a relatively high free volume that minimizes the difference between CO_2 and H_2 diffusivities. One method of increasing CO_2 solubility is the incorporation of protonated amines within the membrane.[11,12] In this case, facilitated transport can lead to CO_2/H_2 selectivities over 100, but carrier saturation often limits the application of these systems to low feed pressures (less than 0.05 bar).[13−15] At room temperature, amorphous poly(ethylene glycol) (PEG)-containing membranes exhibit CO_2/H_2 selectivities ranging from 5 to 12, presumably because of quadrupole−dipole interactions between CO_2 and the ether functional groups of PEG.[16−19] Unfortunately, however, crystallization of PEG chains decreases both the permeability and selectivity of such membranes. To overcome this challenge, several studies employed cross-linked, solution-cast, PEG-containing membranes to maintain a high free volume, decrease crystallinity, and increase chemical stability.[7,20−22] In the best case, the cross-linked membranes show CO_2 permeabilities of up to 600 barrers [1 barrer $= 10^{-10}$ cm^3 (STP)·cm/(cm^2·s·cmHg) $= 7.5 \times 10^{-18}$ m^3 (STP)·m/(m^2·s·Pa)] and CO_2/H_2 selectivities of approximately 12 at room temperature.[23]

Nevertheless, the high thickness (> 100 μm) of solution-cast membranes yields a permeance (permeance is defined as flux/Δp) that is too low for practical separations. This work examines the use of atom transfer radical polymerization (ATRP) from porous substrates to create composite membranes with thin (50−500 nm) skins of PEG-containing films that allow selective removal of CO_2 from H_2 streams. ATRP is attractive for synthesizing these membrane skins because it often affords control over film thickness along with polymer chains with relatively low polydispersity.[24,25] Scheme 1 shows two permutations of the ATRP process for forming membrane skins on porous alumina substrates, and similar processes on porous polymer supports are also possible. Initiator attachment occurs either via adsorption of a disulfide initiator to gold-coated alumina to generate A (scheme 1), or attachment of a silane directly to the alumina to generate B. Subsequent atom transfer radical polymerization with a Cu^+/1,1,4,7,10,10-hexamethyltriethylenetetramine (HMTETA) catalyst yields membrane skins. Because of the small thicknesses of the skins, the permeances of modified alumina membranes are several orders of magnitude greater than those of solution-cast membranes.[8]

Additionally, this work examines the use of copolymers prepared from poly(ethylene glycol methyl ether methacrylate) (PEGMEMA) monomers with different PEG chain lengths (Scheme 2) to inhibit the crystallization of the PEG side chains. The combination of monomers with 8−9 and 23−24 ethylene oxide repeat units yields films that do not crystallize over many months and membrane skins with a room temperature CO_2/H_2 selectivity of around 12.

Experimental Section

Chemicals. PEGMEMA monomers with M_n = 300 Da (PEGMEMA-300), M_n = 475 Da (PEGMEMA-475), and M_n = 1,100 Da (PEGMEMA-1100) were obtained from Aldrich. These monomers contain both 100 ppm 4-methoxyphenol and 300 ppm 2,6-di-*tert*-butyl-4-methylphenol as inhibitors. Proton NMR spectra (see Supporting Information) showed that the average numbers of ethylene oxide units in PEGMEMA-300, PEGMEMA-475, and PEGMEMA-1100 were 4.4, 8.8, and 23.1, respectively. In some cases, the inhibitors were removed from the monomers using flash column chromatography with basic alumina, but this did not have a significant effect on polymerizations, so in most reactions the monomers were used as received. The CuCl, $CuBr_2$, and 1,1,4,7,10,10-hexamethyltriethylenetetramine (HMTETA) were purchased from Aldrich, and deionized water was obtained using a Millipore system (Milli-Q, 18.2 MΩ·cm). THF was distilled over sodium metal with benzophenone, and DMF was distilled over 4 Å molecular sieves. Silicon(100) wafers were obtained from NOVA Electronic

(11) Matsuyama, H.; Teramoto, M.; Matsui, K.; Kitaura, Y. *J. Appl. Polym. Sci.* **2001**, *81*, 936–942.
(12) Matsuyama, H.; Teramoto, M.; Sakakura, H.; Iwai, K. *J. Membr. Sci.* **1996**, *117*, 251–260.
(13) Kim, M.; Park, Y.; Youm, K.; Lee, K. *J. Membr. Sci.* **2004**, *245*, 79–86.
(14) Noble, R. D.; Pellegrino, J. J.; Grosgogeat, E.; Sperry, D.; Way, J. D. *Sep. Sci. Technol.* **1988**, *23*, 1595–1609.
(15) Way, J. D.; Noble, R. D. I. Facilitated Transport. In *Membrane Handbook*; Ho, W. S. W., Sirkar, K. K., Eds.; Van Nostrand Reinhold: New York, 2001; pp 833−866.
(16) Koros, W. J. *J. Polym. Sci., Part B* **1985**, *23*, 1611–1628.
(17) Zhong, J.; Lin, G.; Wen, W.-Y.; Jones, A. A.; Kelman, S.; Freeman, B. D. *Macromolecules* **2005**, *38*, 3754–3764.
(18) Bondar, V. I.; Freeman, B. D.; Pinnau, I. *J. Polym. Sci., Part B* **2000**, *38*, 2051–2062.
(19) Kusuma, V. A.; Matteucci, S.; Freeman, B. D.; Danquah, M. K.; Kalika, D. S. *J. Membr. Sci.* **2009**, *341*, 84–95.
(20) Patel, N. P.; Miller, A. C.; Spontak, R. J. *Adv. Funct. Mater.* **2004**, *14*, 699–707.
(21) Kalakkunnath, S.; Kalika, D. S.; Lin, H.; Freeman, B. D. *Macromolecules* **2005**, *38*, 9679–9687.
(22) Priola, A.; Gozzelino, G.; Ferrero, F.; Malucelli, G. *Polymer* **1993**, *34*, 3653–3657.
(23) Lin, H.; Freeman, B. D.; Kalakkunnath, S.; Kalika, D. S. *J. Membr. Sci.* **2007**, *291*, 131–139.
(24) Balachandra, A. M.; Baker, G. L.; Bruening, M. L. *J. Membr. Sci.* **2003**, *227*, 1–14.
(25) Sun, L.; Baker, G. L.; Bruening, M. L. *Macromolecules* **2005**, *38*, 2307–2314.

Scheme 2. Copolymerization of PEGMEMA-475 and PEGMEMA-1100 to Provide a Membrane Skin

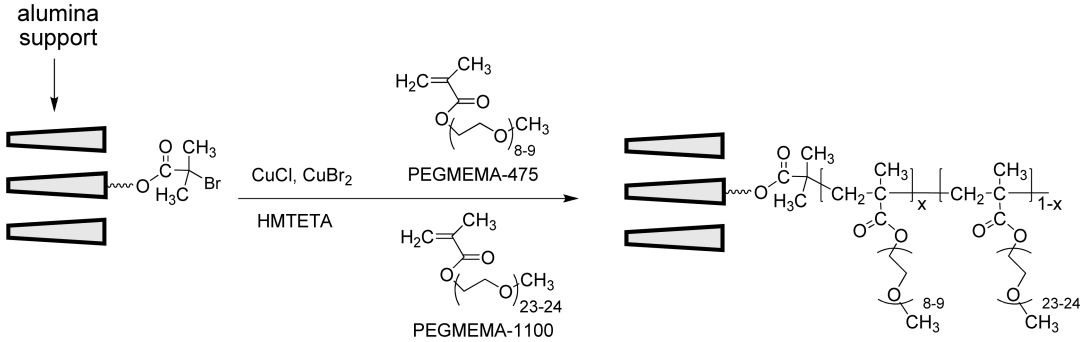

Materials and sputter-coated with 20 nm of chromium followed by 200 nm of gold by LGA Thin Films (Santa Clara, CA). The porous alumina substrates were Anodisc membrane filters (25 mm disks with 0.02 μm surface pores) purchased from Whatman, and the disulfide, $[Br-C(CH_3)_2-COO(CH_2)_{11}S]_2$, and silane, $SiCl(CH_3)_2(CH_2)_{11}OCOC(CH_3)_2Br$, initiators were synthesized as described previously.[26−29]

Polymerization. Porous alumina substrates were initially rinsed with ethanol, dried with N_2, UV/O_3 cleaned (Boekel UV-Clean model 135500) for 15 min, and sputter coated with 5 nm of gold in a Pelco SC-7 sputter coater. The thickness of the gold coating was monitored with a Pelco FTM-2 quartz crystal microbalance. Attachment of a monolayer of the disulfide initiator to gold-coated silicon wafers or porous alumina occurred during an overnight immersion of the substrate in an ethanolic solution containing 1 mM disulfide initiator. The resulting sample was rinsed with 5 mL of ethanol and dried in a N_2 stream. Attachment of the silane initiator occurred during overnight immersion of an uncoated, UV/ozone-cleaned porous alumina substrate in a solution containing 8 mM silane in THF. The resulting sample was rinsed with 5 mL THF and dried in a N_2 stream. The two different types of initiator-modified membranes were handled identically in the ensuing polymerization steps.

Following a previous procedure, the catalyst stock solution was prepared by first dissolving 0.06 g (0.6 mmol) of CuCl and 0.04 g (0.2 mmol) of $CuBr_2$ in 30.0 mL of distilled, degassed DMF.[30,31] This solution was further degassed via three freeze, pump, thaw cycles. In a N_2-filled glovebag, 490 μL (1.8 mmol) of degassed 1,1,4,7,10,10-hexamethyltriethylenetetramine (HMTETA) ligand was added to this solution, which subsequently turned a dark green color during several hours of stirring. During this initial stirring, a small amount of material precipitated, but the resulting catalytic activity of the solution remained constant for at least several weeks. The nominal mole ratio of Cu^+/Cu^{2+}/HMTETA was 3:1:9.

The monomer solution, which contained 0.75 M PEGMEMA in water, was initially degassed via three freeze, pump, thaw cycles. (When different molecular weight monomers were used, the total monomer concentration was maintained at 0.75 M.) The polymerization solution was prepared in a N_2-filled glovebag by combining degassed monomer and catalyst solutions in a 9:1 volume ratio to produce a blue−green solution containing 0.67 M monomer, 2.0 mM CuCl, 0.60 mM $CuBr_2$, and 6.0 mM HMTETA. The initiator-modified membranes or wafers were immersed in the polymerization solution for designated periods of time, and the resulting polymer films were rinsed with 5 mL of water and soaked in water for at least 2 h before rinsing with 5 mL of ethanol and drying under a N_2 stream.

Characterization Methods. Reflectance FT-IR spectroscopy was performed using a Nicolet Magna-IR 560 spectrometer with a Pike grazing angle (80°) attachment. A UV/ozone-cleaned, gold-coated silicon wafer was used to obtain the background spectrum. Thicknesses of films formed on gold-coated silicon were determined with a rotating analyzer ellipsometer (J.A. Woollam model M44) at an incident angle of 75°. A two-term Cauchy equation was employed to simultaneously fit film thickness and the Cauchy constants needed to model the wavelength-dependence of the film refractive index. Thicknesses were determined at a minimum of three locations on each substrate. Scanning electron microscopy was performed with the JEOL semi-in-lens cold cathode field-emission scanning electron microscope, model JSM-7500F, operating with a r-filter in signal maximum mode. Samples were sputter coated with 5 nm of gold prior to imaging.

Gas Permeation. Single gas permeation experiments were performed by exposing the membrane to individual gases at varying pressures in an Advantec/MFS UHP-25 cell with a pressure relief valve. The gas flow rate through the membrane was measured with either an Optiflow 420 electronic soap bubble meter or a manual soap bubble meter. Mixed-gas experiments were performed by loading the membrane into a custom membrane holder (all connections utilized Swagelok fittings and were tested to ensure that they maintained pressure over a time-scale longer than the experiment) that allowed cross-flow of the feed gas as well as a sweep gas on the permeant side. A backpressure valve was employed to sustain the feed gas pressure, and the feed flow rate was high enough to maintain constant composition at the face of the membrane (the stage-cut, or ratio of permeant flow to feed flow, was $<1\%$). The N_2 sweep gas/permeant stream was connected to an automated six-port injector valve on a Hewlett-Packard 6890 GC equipped with a thermal conductivity detector (TCD) and an Agilent GS-CarbonPLOT capillary column (i.d. = 0.53 mm, length = 30 m, 3 μm coating). The mixed gas permeances as well as pure gas permeances were calculated from GC results using eq 3

$$\text{Permeance} = \frac{\chi_B \times \Phi_{N_2}}{\chi_{N_2} \times A \times \Delta p} \quad (3)$$

(26) Shah, R. R.; Merreceyes, D.; Husemann, M.; Rees, I.; Abbott, N. L.; Hawker, C. J.; Hedrick, J. L. *Macromolecules* **2000**, *33*, 597–605.
(27) Zheng, Y.; Bruening, M. L.; Baker, G. L. *Macromolecules* **2007**, *40*, 8212–8219.
(28) Matyjaszewski, K.; Miller, P. J.; Shukla, N.; Immaraporn, B.; Gelman, A.; Luokala, B. B.; Siclovan, T. M.; Kickelbick, G.; Vallant, T.; Hoffmann, H.; Pakula, T. *Macromolecules* **1999**, *32*, 8716–8724.
(29) Bao, Z.; Bruening, M. L.; Baker, G. L. *Macromolecules* **2006**, *39*, 5251–5258.
(30) Kim, J.-B.; Huang, W.; Miller, M. D.; Baker, G. L.; Bruening, M. L. *J. Polym. Sci., Part A* **2003**, *41*, 386–394.
(31) Cheng, N.; Azzaroni, O.; Moya, S.; Huck, W. T. S. *Macromol. Rapid Commun.* **2006**, *27*, 1632–1636.

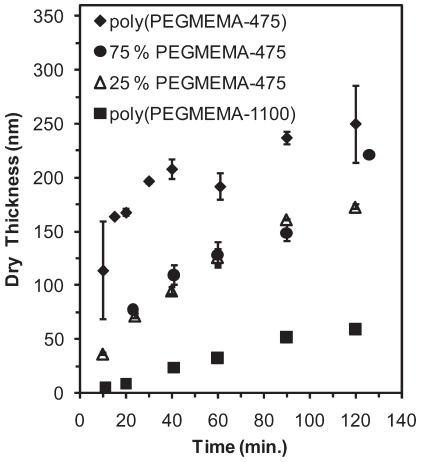

Figure 1. Evolution of film thickness with time in surface-initiated polymerization of pure and mixed monomer solutions. For copolymers, the legend shows the solution PEGMEMA-475 mol percentage with respect to the total monomer (PEGMEMA-475 plus PEGMEMA-1100). The overall monomer concentration was 0.67 M, and the catalyst system was 2.0 mM CuCl, 0.60 mM $CuBr_2$, and 6.0 mM HMTETA. The error bars, which in many cases are obscured by the symbols, represent one standard deviation.

where χ_B is the mole fraction of a particular permeate gas, B, in the gas mixture injected into the GC column, Φ_{N_2} is the sweep gas flow rate, χ_{N_2} is the mole fraction of N_2 in the gas injected into the GC column, Δp is the transmembrane partial pressure difference for the gas of interest, and A is the membrane area. (Φ_{N_2}/χ_{N_2} is the sum of the permeate and sweep gas flow rate, and χ_{N_2} was determined by subtracting the mole fractions of the permeates from unity. This assumes that the amount of N_2 passing from permeate to feed was negligible.) The sweep gas flow rate was programmed into a mass flow controller, pressure and area were measured, and the mole fractions were determined from the integrated GC spectra and a calibration curve.

Results and Discussion

Polymerization Rates as a Function of Monomer Composition. The first step in developing surface-initiated ATRP for creating membrane skins, especially for forming copolymer skins, is examination of polymerization from model flat substrates such as gold-coated silicon wafers.[32] Such substrates facilitate ellipsometric and spectroscopic characterization of polymer growth and composition. We are particularly interested in the relative film growth rates for PEGMEMA-475, PEGMEMA-1100, and their mixtures[33] because the short side chains of PEGMEMA-475 do not crystallize, whereas the long chains of PEGMEMA-1100 should promote CO_2/H_2 selectivity. As Figure 1 shows, polymerization of PEGMEMA-475 by itself gives the most rapid initial growth in film thickness, but the growth rate decreases dramatically after 15 min of polymerization. In contrast, polymerization of PEGMEMA-1100 is slower, but the film growth rate is essentially constant for 120 min. Interestingly, surface-initiated polymerizations of mixtures in which

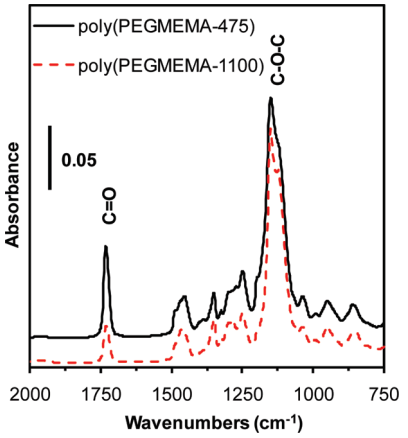

Figure 2. FTIR spectra of 152 nm-thick poly(PEGMEMA-475) (black line) and 118 nm-thick poly(PEGMEMA-1100) (dashed red line) films on gold-coated substrates. Spectra were taken immediately after polymerization before the PEG side chains in poly(PEGMEMA-1100) crystallized. The spectra are offset for clarity.

PEGMEMA-475 constitutes either 25 or 75 mol % of the total monomer show relatively high and steady growth rates.

Decreases in growth rates with polymerization time, particularly for poly(PEGMEMA-475), suggest that the HMTETA-$Cu^{+/2+}$ catalyst system gives a high concentration of radicals that results in significant termination by radical−radical coupling. The large side chains of PEGMEMA-1100 may provide steric hindrance to both polymerization and termination. In solution polymerization studies, Lad et al. attributed the high ATRP activity of PEGMEMA-475 relative to PEGMEMA-1100 to ethylene oxide coordination with the Cu catalyst in close proximity to the double bond.[34] However, steric issues seem equally likely to affect polymerization.[33] In the case of homopolymerization from surfaces, the PEGMEMA-1100 solutions are also more viscous and contain less water than PEGMEMA-475 solutions, and both of these factors should also lead to lower polymerization rates for the PEGMEMA-1100. Mixtures of PEGMEMA-475 and PEGMEMA-1100 have intermediate polymerization rates, and the side chains are apparently still sufficiently large to reduce termination relative to pure PEGMEMA-475. For PEGMEMA-475, PEGMEMA-1100, and their mixtures, film growth is rapid compared to polymerization of most other monomers and nonaqueous polymerizations.[35−37] A number of studies demonstrated that the presence of water frequently enhances the rate of ATRP.[35−39]

Determining the Composition of Copolymer Films. The molar ratio of PEGMEMA-475 to PEGMEMA-1100 in

(32) Zhou, F.; Zheng, Z.; Yu, B.; Liu, W.; Huck, W. T. S. *J. Am. Chem. Soc.* **2006**, *128*, 16253–16258.
(33) Brown, A. A.; Khan, N. S.; Steinbock, L.; Huck, W. T. S. *Eur. Polym. J.* **2005**, *41*, 1757–1765.
(34) Lad, J.; Harrisson, S.; Haddleton, D. M. *Mechanistic Aspects of Copper-mediated Living Radical Polymerization*; American Chemical Society: Washington, DC, 2003; Vol. *854*, pp 148−160.
(35) Huang, W.; Kim, J.-B.; Bruening, M. L.; Baker, G. L. *Macromolecules* **2002**, *35*, 1175–1179.
(36) Wang, X. S.; Armes, S. P. *Macromolecules* **2000**, *33*, 6640–6647.
(37) Wang, X. S.; Lascelles, S. F.; Jackson, R. A.; Armes, S. P. *Chem. Commun.* **1999**, 1817–1818.
(38) Jain, P.; Dai, J.; Grajales, S.; Saha, S.; Baker, G. L.; Bruening, M. L. *Langmuir* **2007**, *23*, 11360–11365.
(39) Tsarevsky, N. V.; Matyjaszewski, K. *Chem. Rev.* **2007**, *107*, 2270–2299.

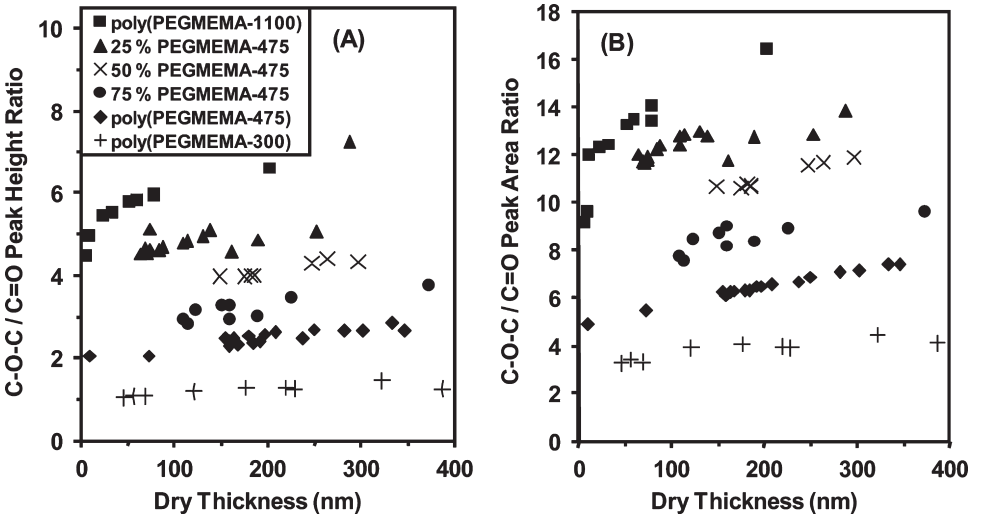

Figure 3. Ratios of C−O−C to C=O peak heights (A) and peak areas (B) in reflectance FTIR spectra of poly(PEGMEMA-1100), poly(PEGMEMA-475), poly(PEGMEMA-300), and poly(PEGMEMA-475-*co*-PEGMEMA-1100) films on gold-coated substrates. The ratios are plotted as a function of the ellipsometric thickness of the film, and for the copolymers, the legend shows the mole fraction of PEGMEMA-475 (relative to total monomer) in the polymerization solution. All polymerizations employed a total monomer concentration of 0.67 M, and the Experimental Section describes the polymerization conditions.

a film may not correspond to the monomer ratio in the polymerization solution. In particular, the smaller monomer may be more reactive because of faster diffusion to the surface or less steric hindrance to polymerization. In an attempt to determine the relative amounts of each monomer incorporated in poly(PEGMEMA-475-*co*-PEGMEMA-1100) films, we compared the intensities of carbonyl (1731 cm^{-1}) and C−O−C (1149 cm^{-1}) absorbances in both homopolymer and copolymer films. The reflectance FTIR spectra in Figure 2 show that for amorphous homopolymer films, the intensity of the C−O−C stretch relative to the C=O stretch is much higher for poly(PEGMEMA-1100) than poly(PEGEMEMA-475), as would be expected because of the longer PEG chain in the higher molecular weight monomer.

We initially planned to estimate the mole ratios of monomers incorporated into a copolymer film using eq 4, where x_{475} is the mole fraction of PEGMEMA-475 in a copolymer film and R_{co}, R_{1100}, and R_{475} are the ratios of the C−O−C peak height (1149 cm^{-1}) to the C=O peak height (1731 cm^{-1}) for copolymer, poly(PEGMEMA-1100), and poly(PEGMEMA-475) films, respectively.

$$R_{co} = x_{475}R_{475} + (1 - x_{475})R_{1100} \qquad (4)$$

However, Figure 3 suggests that in some cases peak height and peak area ratios for the C−O−C to C=O absorbance increase with film thickness for homopolymer and copolymer films. This increasing ratio of C−O−C to C=O absorbance likely occurs because reflectance measurements plot $\log(R_o/R)$, where R_o and R are the reflectivities of bare and film-covered substrates, respectively. These reflectivities are complicated functions of the film thickness and the complex refractive indices, $\tilde{n} = n - ik$, of the substrate and the film. To account for these complications in reflectance FTIR spectroscopy, we performed Fresnel calculations

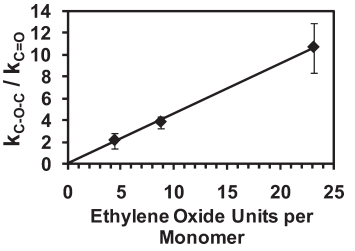

Figure 4. Ratios of C−O−C (1149 cm^{-1}) and C=O (1731 cm^{-1}) absorption coefficients, k, as a function of the average number of ethylene oxide units per repeat unit, EO_{avg}, in poly(PEGMEMA-300), poly(PEGMEMA-475), and poly(PEGMEMA-1100) films. The ethylene oxide units per monomer were calculated from ^{1}H NMR spectra of monomers, and the standard deviations in the absorption coefficient ratios were determined using films with thicknesses ranging from 5 to 454 nm. The line is a fit to the data with a zero intercept.

Table 1. Composition of Poly(PEGMEMA-475-*co*-PEGMEMA-1100) Films[a] as a Function of the PEGMEMA-475 mol Percentages in the Polymerization Solution[b]

feed solution, mole% PEGMEMA-475	polymer composition, mole% PEGMEMA-475	EO_{avg}
0	0	23 ± 1
25	33 ± 2	18 ± 1
50	54 ± 3	15 ± 1
75	71 ± 7	13 ± 1
100	100	8.7 ± 0.6

[a] Film compositions were determined from reflectance FTIR spectra and Fresnel calculations (see text) and are expressed as both mole percent and the average number of ethylene oxide (EO_{avg}) groups per repeat unit. The uncertainties, which were calculated using propagation of error, represent one standard deviation. [b] The mole percentage in the feed solution is relative to the total amount of monomer in solution.

to determine the absorption coefficient, k, for different films at the wavelengths of interest. The Supporting Information provides the details of these calculations and shows that the calculated absorption coefficients do not vary significantly with the thicknesses of the films (Figure S2). We used the k values for three homopolymer films, poly(PEGMEMA-300), poly(PEGMEMA-475),

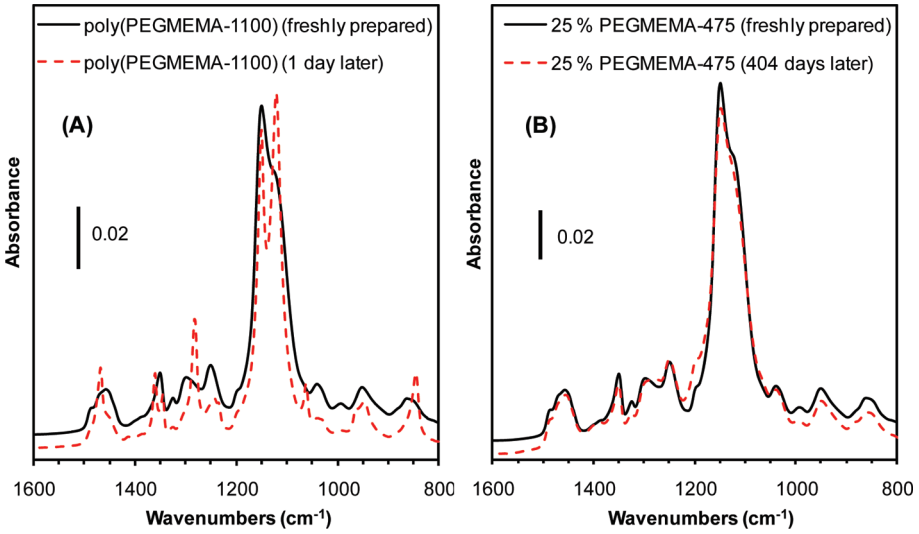

Figure 5. Reflectance FTIR spectra of (A) 60-nm-thick poly(PEGMEMA-1100) immediately after polymerization (solid black line) and 24 h later (dashed red line) and (B) 97-nm-thick poly(PEGMEMA-475-*co*-PEGMEMA-1100) immediately after polymerization (solid black line) and 404 days later (dashed red line). The copolymer was prepared from a solution containing 25 mol % PEGMEMA-475 and 75 mol % PEGMEMA-1100.

and poly(PEGMEMA-1100), to create a calibration curve (Figure 4) of the $k_{C-O-C}/k_{C=O}$ ratio versus the average number of ethylene oxide units per repeat unit, EO_{avg}, and then calculated EO_{avg} in copolymer films. For poly(PEGMEMA-475-*co*-PEGMEMA-1100), this EO_{avg} value is a direct function of the fraction of each monomer in the copolymer and the average number of ethylene oxide units in each monomer (eq 5).

$$EO_{avg} = 8.8x_{475} + 23.1(1 - x_{475}) \quad (5)$$

The reflectance FTIR data and the Fresnel calculations show that the ratios of PEGMEMA-475 to PEGMEMA-1100 in poly(PEGMEMA-475-*co*-PEGMEMA-1100) films are approximately the same as those in the solutions from which they grow (Table 1). This is somewhat surprising considering the large differences in the initial growth rates as well as termination rates for surface-initiated homopolymerization of the two monomers (Figure 1). However, in the case of copolymers, solutions containing 25 mol % and 75 mol % PEGMEMA-475 give essentially the same initial growth rate (Figure 1), which is consistent with the similarity between solution and film compositions. This direct correlation between solution and film compositions affords straightforward control over the ratio of long and short side chains to minimize PEG crystallization and maximize CO_2/H_2 selectivity in membranes.

Crystallization of PEG Side Chains. PEG chains crystallize in helices that contain two turns per 7 EO units over a length of 19.3 Å,[40−42] and helix formation leads to splitting of the 1150 cm^{-1} C−O−C IR band into peaks at 1120 and 1148 cm^{-1} and a narrowing of the CH_2 wagging peak at 1360 cm^{-1}.[40,41] In PEGMEMA films, long PEG side chains crystallize similarly, and Figure 5A demonstrates the changes in reflectance FTIR spectra that occur upon crystallization of a poly(PEGMEMA-1100) film. Previous reports of PEG crystallization in related coatings suggest that the helical axis preferentially orients perpendicular to the surface in films less than 100 nm thick, and both perpendicular and parallel to the surface in thicker films.[27,43−46]

However, the presence of crystallinity, rather than its orientation, is the primary concern for creating selective membranes with high permeabililties, and prior studies reveal that the PEG chain length, not film thickness, is the primary factor in determining whether crystallization occurs.[47,48] In contrast to poly(PEGMEMA-1100), poly(PEGMEMA-475) films do not show any evidence of crystallization in reflectance FTIR spectra, presumably because neighboring PEG side chains are too short to crystallize in this environment.[49]

Importantly, copolymers prepared from PEGMEMA-1100 and PEGMEMA-475 show no sign of crystallization, even when the fraction of PEGMEMA-475 in the film is only ~25%. Figure 5B shows that the reflectance FTIR spectrum of a poly(PEGMEMA-475-*co*-PEGMEMA-1100) film remains unchanged even after more than a year at room temperature. The presence of the short chains is apparently sufficient to inhibit crystallization of the longer side chains, and this effect occurs for films prepared from solutions containing PEGMEMA-475 as 25, 50, and 75 mol % of the total monomer.

Formation of Gas-Separation Membranes by ATRP. Composite membranes are attractive for gas separations

(40) Miyazawa, T.; Ideguchi, Y.; Fukushima, K. *J. Chem. Phys.* **1962**, *37*, 2764–2776.
(41) Yoshihara, T.; Murahashi, S.; Tadokoro, H. *J. Chem. Phys.* **1964**, *41*, 2902–2911.
(42) Takahashi, Y.; Tadokoro, H. *Macromolecules* **1973**, *6*, 672–675.
(43) Li, X.; Hsu, S. L. *J. Polym. Sci., Part B* **1984**, *22*, 1331–1342.
(44) Schönherr, H.; Frank, C. W. *Macromolecules* **2003**, *36*, 1188–1198.
(45) Schönherr, H.; Frank, C. W. *Macromolecules* **2003**, *36*, 1199–1208.
(46) Wang, H. P.; Keum, J. K.; Hiltner, A.; Baer, E.; Freeman, B.; Rozanski, A.; Galeski, A. *Science* **2009**, *323*, 757–760.
(47) Bitter, J. G. A. *Desalination* **1984**, *51*, 19–35.
(48) Preston, W. E.; Barlow, J. W.; Paul, D. R. *J. Appl. Polym. Sci.* **1984**, *29*, 845–852.
(49) Lin, H.; Kai, T.; Freeman, B. D.; Kalakkunnath, S.; Kalika, D. S. *Macromolecules* **2005**, *38*, 8381–8393.

because the minimal thickness of the thin, selective skin allows for high flux, and the underlying support provides mechanical strength. Hence, the goal in using ATRP to create a membrane skin is to completely cover a porous substrate with a thin film without filling the underlying pores. The first step in the formation of membranes by ATRP is attachment of an initiator to the surface. To be consistent with our work on gold wafers, we sputtered 5 nm of gold on porous alumina and subsequently adsorbed a monolayer of the disulfide initiator on the surface (Scheme 1A). In a separate procedure, to avoid the deposition of gold on the membrane surface, we attached a silane initiator directly to the alumina (Scheme 1B). Because alumina membranes are expensive and fragile, we are also working on growing membrane skins on polymeric ultrafiltration membranes. This is more challenging, however, because the solvents employed in initiator attachment may damage the underlying membrane. Aqueous adsorption of macroinitiators may overcome this problem.[38]

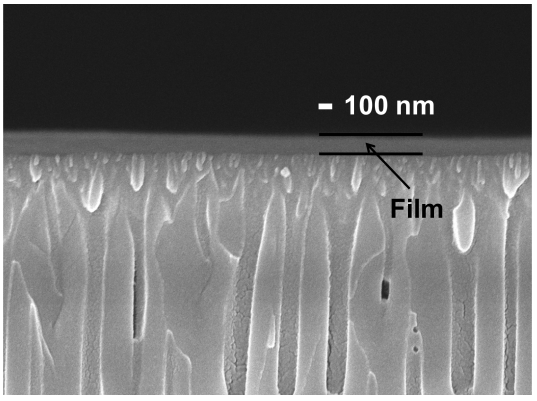

Figure 6. SEM image of the cross section of a gold-coated porous alumina membrane modified with a poly(PEGMEMA-475-*co*-PEGMEMA-1100) film. The alumina exhibits unfilled vertical pores covered by a 130-nm-thick film that was grown from an aqueous solution containing 25 mol % PEGMEMA-475 and 75 mol % PEGMEMA-1100.

Subsequent polymerization of PEGMEMA from initiators on alumina yields the desired composite membranes. Figure 6 shows a SEM image of a composite membrane containing a poly(PEGMEMA-475-*co*-PEGMEMA-1100) skin on a porous alumina support. The film is thin (130 nm) and clearly covers the pores without filling them. However, selective gas permeation studies are needed to demonstrate that the films are defect-free and noncrystalline.

Gas Permeation through Poly(PEGMEMA) Membranes. Figure 7 shows the CO_2 and H_2 fluxes through porous alumina membranes coated with either a poly(PEGMEMA-1100) film or a copolymer film grown from a solution containing a 1:1 mol ratio of PEGMEMA-475 and PEGMEMA-1100. For poly(PEGMEMA-1100), the initial CO_2/H_2 selectivity is 12 ± 1. The highest room-temperature CO_2/H_2 selectivity of PEG-containing membranes in the literature is also 12.[7,21−23] However, the CO_2/H_2 selectivity of the poly(PEGMEMA-1100) film drops to less than 1 within a day because the CO_2 flux decreases 12-fold. This drop in CO_2 flux is almost certainly due to crystallization of the PEG side chains, which as noted above occurs within one day of synthesis of poly(PEGMEMA-1100) films.

By comparison, poly(PEGMEMA-475) films exhibit an initial CO_2/H_2 selectivity of 9 ± 2. On silylated supports, poly(PEGMEMA-1100) and poly(PEGMEMA-475) films show selectivities of 13 ± 1 and 5.8 ± 0.5, respectively, demonstrating that there is a significant difference between the gas selectivities of these two polymers. The poly(PEGMEMA-475) films contain a smaller overall fraction of PEG than poly(PEGMEMA-1100), which likely explains their lower selectivity. However, the selectivity of the poly(PEGMEMA-475) does not decrease with time because the shorter chains do not crystallize.

The goal of using copolymers as membranes is to achieve the initial selectivity of poly(PEGMEMA-1100)

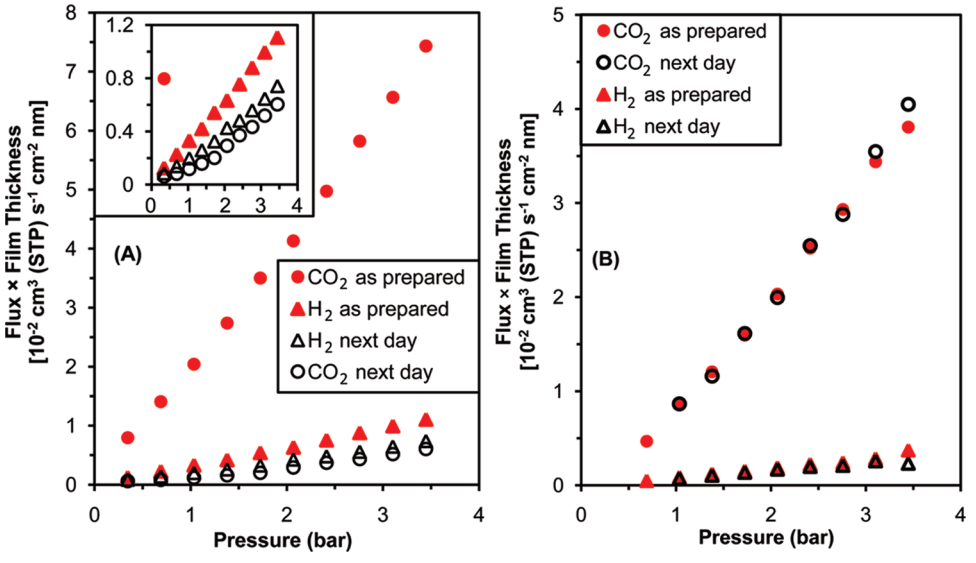

Figure 7. Single-gas fluxes through gold-coated porous alumina membranes capped with (A) poly(PEGMEMA-1100) or (B) poly(PEGMEMA-475-*co*-PEGMEMA-1100) grown from a solution containing 50 mol % PEGMEMA-475. (Fluxes are normalized by multiplying by the SEM thickness of the membrane skin.) The circles represent CO_2 data, and the triangles represent H_2 data; filled symbols represent measurements taken immediately after synthesis, and open symbols represent data obtained 24 h later. The inset in Figure A shows the data on an expanded ordinate for clarity.

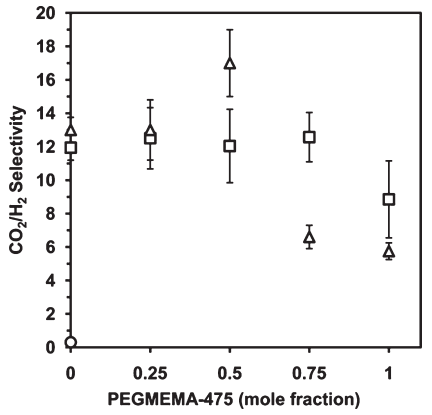

Figure 8. Single-gas CO_2/H_2 selectivity vs mole fraction of PEGMEMA-475 in the monomer solution used to create amorphous poly(PEGMEMA-475-*co*-PEGMEMA-1100) films on porous alumina membranes. The triangles represent films grown from silylated alumina and the squares represent films grown from initiators on gold-coated alumina. For the poly(PEGMEMA-1100) homopolymer on silylated alumina, the open circle near the origin represents selectivity after crystallization. Error bars are one standard deviation.

films while avoiding decreases in selectivity and flux due to film crystallization. Figure 7B shows that a poly(PEGMEMA-475-*co*-PEGMEMA-1100) film (prepared on gold-coated alumina using a solution containing 50 mol % PEGMEMA-475) has an initial CO_2/H_2 selectivity of 12−13, which is essentially the same as that of the pure poly(PEGMEMA-1100). Moreover, the selectivity of the copolymer membranes is constant over at least several weeks at room temperature, again presumably because the side chains of PEGMEMA-475 inhibit crystallization. Figure 8 shows the dependence of CO_2/H_2 selectivity on the mole fraction of PEGMEMA-475 in poly(PEGMEMA-475-*co*-PEGMEMA-1100) films. As long as there is 75 mol % or less PEGMEMA-475 in the polymerization solution, membranes formed on gold-coated alumina maintain average CO_2/H_2 selectivities of 12 at room temperature. The films grown from silylated alumina show a maximum CO_2/H_2 selectivity of 17 ± 2 with copolymers generated from a 50 mol % PEGMEMA-475 polymerization solution, but a selectivity of only 7 when using 75 mol % PEGMEMA-475. Silanization is more likely to produce initiators within the pores of the alumina, which might somewhat alter film structure at the support surface and change selectivity relative to films on gold-coated alumina. Moreover, the initiator packing densities might be different for the gold-coated and silylated surfaces.

Determination of the permeability, P, of the films on porous alumina is challenging because of the difficulty in obtaining accurate values for film thickness (see eq 1). Film thicknesses in multiple cross-sectional SEM images of a given membrane typically show a relative standard deviation (rsd) of 10−30%, although sometimes we see even larger variations. Based on SEM images of membranes with a rsd in thickness $< 25\%$, the H_2 permeability of poly(PEGMEMA-475-*co*-PEGMEMA-1100) films ranges from 2 to 6 barrers, and the CO_2 permeability ranges from 20 to 60 barrers. (Given the uncertainty in thickness, we could not differentiate among permeabilities of films with different compositions.) Typical CO_2 permeabilities of PEG-containing films range from 12 barrers in pure PEG[50] to 570 barrers in cross-linked PEG-based acrylates.[49,51] This wide range of permeabilities in different PEG-containing polymers stems from differences in fractional free volume and the presence of different polar groups that alter the solubility of gases in the membrane.[23,52,53] Although the poly(PEGMEMA-475-*co*-PEGMEMA-1100) films do not exhibit as high a permeability as some cross-linked films, the ultrathin skin maximizes permeance for a given permeability. To improve permeability, future studies will examine cross-linking to increase flux in these films.

Selectivities in gas mixtures can differ significantly from those with single gases, particularly when absorption of a gas such as CO_2 plasticizes the membranes.[54] In mixed-gas experiments, plasticization may increase the flux of H_2 and decrease CO_2/H_2 selectivity relative to single-gas measurements. With feed gas streams of 79.7 mol % H_2 and 20.3 mol % CO_2, the CO_2/H_2 selectivity was only 13% lower on average than the pure gas CO_2/H_2 selectivities.

Summary

In their amorphous state, composite poly(PEGMEMA-1100) membranes provide high CO_2 permeances and CO_2/H_2 selectivities, but crystallization can decrease flux by an order of magnitude and reduce CO_2/H_2 selectivity to below 1. Copolymerization of two PEGMEMA monomers, one containing 8−9 and the other 23−24 ethylene oxide units per side chain, avoids the problem of crystallization and yields films that maintain an amorphous state for more than a year. Reflectance FTIR spectra indicate that the ratio of the PEGMEMA-475 and PEGMEMA-1100 incorporated into copolymer films is within 8% of the ratio of the monomers in the polymerization solution. Membranes consisting of porous alumina supports coated with copolymer films exhibit stable single-gas CO_2/H_2 selectivities around 12 at room temperature, which is attractive for CO_2 removal from H_2 streams.

Acknowledgment. We thank the U.S. Department of Energy Office of Basic Energy Sciences for funding and S. Koszalka and Dr. Kathryn Severin for their assistance.

Supporting Information Available: Details of the method used to calculate absorption coefficients from reflectance FTIR spectra, values for these coefficients, and proton NMR spectra of monomers. This material is available free of charge via the Internet at http://pubs.acs.org.

(50) Lin, H.; Freeman, B. D. *J. Membr. Sci.* **2004**, *239*, 105–117.
(51) Lin, H.; Freeman, B. D. *Macromolecules* **2005**, *38*, 8394–8407.
(52) Lin, H.; Freeman, B. D. *J. Mol. Struct.* **2005**, *739*, 57–74.
(53) Kelman, S. D.; Raharjo, R. D.; Bielawski, C. W.; Freeman, B. D. *Polymer* **2008**, *49*, 3029–3041.
(54) White, L. S.; Blinka, T. A.; Kloczewski, H. A.; Wang, I.-f. *J. Membr. Sci.* **1995**, *103*, 73–82.